

EVOLUTION OF RELATIVISTIC POLYTROPES IN THE POST-QUASI-STATIC REGIME

L. Herrera ^{1 2} and W. Barreto ³

Abstract

A recently presented method for the study of evolving self-gravitating relativistic spheres is applied to the description of the evolution of relativistic polytropes. Two different definitions of relativistic polytrope, yielding the same Newtonian limit, are considered. Some examples are explicitly worked out, describing collapsing polytropes and bringing out the differences between both types of polytropes.

Key words: Relativistic polytropes; post-quasi-static regime

¹Escuela de Física, Facultad de Ciencias, Universidad Central de Venezuela, Caracas, Venezuela.

²Postal address: Apartado Postal 80793, Caracas 1080A, Venezuela. e-mail: laherrera@telcel.net.ve

³Grupo de Física Teórica, Departamento de Física, Facultad de Ciencias, Universidad de los Andes, Mérida, Venezuela. e-mail: wbarreto@ula.ve

1 Introduction

The use of polytropic equations of state in the study of the stellar structure has long and a venerable history [1, 2, 3] (and references therein). Its great success stems, mainly, from its simplicity and from the fact that it can be used to describe a large number of different situations.

It is therefore not surprising that a great deal of work has been devoted to the study of polytropes in the context of general relativity [4, 5, 6, 7] (and references therein). Nevertheless, since the Lane–Emden equation, which is the cornerstone in the study of polytropic spheres, is based on the assumption of hydrostatic equilibrium, almost all works done so far (to our knowledge) on polytropic equations of state, concern spheres in hydrostatic equilibrium (collapsing “Newtonian” polytropes with $n = 3$, have been considered by Goldreich and Weber [8]).

However, during their evolution, self–gravitating objects may pass through phases of intense dynamical activity, with time scales of the order of magnitude of (or even smaller than) the hydrostatic time scale, and for which the static (or the quasi–static) approximation is clearly not reliable (e.g. the collapse of very massive stars [9] and the quick collapse phase preceding neutron star formation [10] (and references therein). In these cases it is mandatory to take into account terms which describe departure from equilibrium. Ac-

cordingly, it is our purpose in this work to study the evolution of polytropes out of hydrostatic equilibrium.

For doing so, we shall make use of an approach for modeling the evolution of self-gravitating spheres, which does not require full numerical integration of time dependent Einstein equations [11]. The motivation for this, is based on the following argument: It is true that numerical methods [12] (and references therein) are enabling researchers to investigate systems which are extremely difficult to handle analytically. In the case of General Relativity, numerical models have proved valuable for investigations of strong field scenarios and have been crucial to reveal unexpected phenomena [13]. Even specific difficulties associated with numerical solutions of partial differential equations in presence of shocks are being overpassed [14]. By these days what seems to be the main limitation for numerical relativity is the computational demands for 3D evolution, prohibitive in some cases [15]. Nevertheless, it is obviously simpler (in general) to solve ordinary than partial differential equations and furthermore purely numerical solutions usually hinder to catch general, qualitative, aspects of the process. Instead, the proposed method, starting from any interior (analytical or numerical) static spherically symmetric (“seed”) solution to Einstein equations, leads to a system of ordinary differential equations for quantities evaluated at the boundary surface of the fluid distribution, whose solution (numerical), allows for modeling the dy-

namics of self-gravitating spheres, whose static limit is the original “seed” solution.

The approach is based on the introduction of a set of conveniently defined “effective” variables, which are effective pressure and energy density, and an heuristic ansatz on the latter [11], whose rationale and justification become intelligible within the context of the post-quasistatic approximation defined below. In the quasistatic approximation (see below), the effective variables coincide with the corresponding physical variables (pressure and density) and therefore the method may be regarded as an iterative method with each consecutive step corresponding to a stronger departure from equilibrium. In this work we shall restrain ourselves to the post-quasistatic level (see section 4 for details).

The fluid distribution under consideration will be assumed to be dissipative. Indeed, dissipation due to the emission of massless particles (photons and/or neutrinos) is a characteristic process in the evolution of massive stars. In fact, it seems that the only plausible mechanism to carry away the bulk of the binding energy of the collapsing star, leading to a neutron star or black hole is neutrino emission [16]. Consequently, in this paper, the matter distribution forming the selfgravitating object will be described as a dissipative fluid, which in the equilibrium regime satisfies a polytropic equation of state.

On the other hand, in the treatment of radiative transfer within stellar objects, two different approximations are usually adopted: diffusion and streaming out.

In the diffusion approximation, it is assumed that the energy flux of radiation (as that of thermal conduction) is proportional to the gradient of temperature. This assumption is in general very sensible, since the mean free path of particles responsible for the propagation of energy in stellar interiors is in general very small as compared with the typical length of the object. Thus, for a main sequence star as the sun, the mean free path of photons at the centre, is of the order of 2 cm . Also, the mean free path of trapped neutrinos in compact cores of densities about $10^{12}\text{ g.cm.}^{-3}$ becomes smaller than the size of the stellar core [17, 18]. Furthermore, the observational data collected from supernovae 1987A indicates that the regime of radiation transport prevailing during the emission process, is closer to the diffusion approximation than to the streaming out limit [19].

However in many other circumstances, the mean free path of particles transporting energy may be large enough as to justify the free streaming approximation. In this work, for simplicity, we shall consider only the streaming out limit.

As we shall see, in the relativistic regime, two (at least) different defini-

tions of polytrope are possible, yielding the same Newtonian limit. We shall consider both of them, as possible “seed” equations of state and we shall contrast the patterns of evolution obtained from each case.

The plan of the paper is as follows. In Section 2 we define the conventions and give the field equations and expressions for the kinematical and physical variables we shall use, in noncomoving coordinates. In Section 3 we present a brief review of the properties of Newtonian polytropes and discuss two possible generalizations to the relativistic regime. A resume of the proposed approach is presented in Section 4. In Section 5 the method is applied to the case when the “seed” equation of state is a relativistic polytrope and some examples are explicitly worked out. Finally a discussion of results is presented in Section 6.

2 Relevant Equations and Conventions

2.1 The field equations

We consider spherically symmetric distributions of collapsing fluid, undergoing dissipation in the form of free streaming radiation, bounded by a spherical surface Σ .

The line element is given in Schwarzschild–like coordinates by

$$ds^2 = e^\nu dt^2 - e^\lambda dr^2 - r^2 (d\theta^2 + \sin^2\theta d\phi^2), \quad (1)$$

where $\nu(t, r)$ and $\lambda(t, r)$ are functions of their arguments. We number the coordinates: $x^0 = t$; $x^1 = r$; $x^2 = \theta$; $x^3 = \phi$. We use geometric units and therefore we have $c = G = 1$.

The metric (1) has to satisfy the Einstein field equations

$$G_\mu^\nu = -8\pi T_\mu^\nu, \quad (2)$$

which in our case read [20]:

$$-8\pi T_0^0 = -\frac{1}{r^2} + e^{-\lambda} \left(\frac{1}{r^2} - \frac{\lambda'}{r} \right), \quad (3)$$

$$-8\pi T_1^1 = -\frac{1}{r^2} + e^{-\lambda} \left(\frac{1}{r^2} + \frac{\nu'}{r} \right), \quad (4)$$

$$\begin{aligned} -8\pi T_2^2 = -8\pi T_3^3 = & -\frac{e^{-\nu}}{4} (2\ddot{\lambda} + \dot{\lambda}(\dot{\lambda} - \dot{\nu})) \\ & + \frac{e^{-\lambda}}{4} \left(2\nu'' + \nu'^2 - \lambda'\nu' + 2\frac{\nu' - \lambda'}{r} \right), \end{aligned} \quad (5)$$

$$-8\pi T_{01} = -\frac{\dot{\lambda}}{r}, \quad (6)$$

where dots and primes stand for partial differentiation with respect to t and r , respectively.

In order to give physical significance to the T_ν^μ components we apply the Bondi approach [20]. Thus, following Bondi, let us introduce purely locally Minkowski coordinates (τ, x, y, z)

$$d\tau = e^{\nu/2} dt; \quad dx = e^{\lambda/2} dr; \quad dy = r d\theta; \quad dz = r \sin\theta d\phi.$$

Then, denoting the Minkowski components of the energy tensor by a bar, we have

$$\bar{T}_0^0 = T_0^0; \quad \bar{T}_1^1 = T_1^1; \quad \bar{T}_2^2 = T_2^2; \quad \bar{T}_3^3 = T_3^3; \quad \bar{T}_{01} = e^{-(\nu+\lambda)/2} T_{01}.$$

Next, we suppose that when viewed by an observer moving relative to these coordinates with proper velocity ω in the radial direction, the physical content of space consists of a fluid of energy density ρ , radial pressure P and unpolarized radiation of energy density $\hat{\epsilon}$ traveling in the radial direction. Thus, when viewed by this (comoving with the fluid) observer the covariant tensor in Minkowski coordinates is

$$\begin{pmatrix} \rho + \hat{\epsilon} & -\hat{\epsilon} & 0 & 0 \\ -\hat{\epsilon} & P + \hat{\epsilon} & 0 & 0 \\ 0 & 0 & P & 0 \\ 0 & 0 & 0 & P \end{pmatrix}.$$

Then a Lorentz transformation readily shows that

$$T_0^0 = \bar{T}_0^0 = \frac{\rho + P\omega^2}{1 - \omega^2} + \epsilon, \quad (7)$$

$$T_1^1 = \bar{T}_1^1 = -\frac{P + \rho\omega^2}{1 - \omega^2} - \epsilon, \quad (8)$$

$$T_2^2 = T_3^3 = \bar{T}_2^2 = \bar{T}_3^3 = -P, \quad (9)$$

$$T_{01} = e^{(\nu+\lambda)/2} \bar{T}_{01} = -\frac{(\rho + P)\omega e^{(\nu+\lambda)/2}}{1 - \omega^2} - e^{(\nu+\lambda)/2} \epsilon, \quad (10)$$

with

$$\epsilon \equiv \hat{\epsilon} \frac{(1 + \omega)}{(1 - \omega)}. \quad (11)$$

Note that the coordinate velocity in the (t, r, θ, ϕ) system, dr/dt , is related to ω by

$$\omega = \frac{dr}{dt} e^{(\lambda-\nu)/2}. \quad (12)$$

Feeding back (7–10) into (3–6), we get the field equations in the form

$$\frac{\rho + P\omega^2}{1 - \omega^2} + \epsilon = -\frac{1}{8\pi} \left\{ -\frac{1}{r^2} + e^{-\lambda} \left(\frac{1}{r^2} - \frac{\lambda'}{r} \right) \right\}, \quad (13)$$

$$\frac{P + \rho\omega^2}{1 - \omega^2} + \epsilon = -\frac{1}{8\pi} \left\{ \frac{1}{r^2} - e^{-\lambda} \left(\frac{1}{r^2} + \frac{\nu'}{r} \right) \right\}, \quad (14)$$

$$P = -\frac{1}{8\pi} \left\{ \frac{e^{-\nu}}{4} (2\ddot{\lambda} + \dot{\lambda}(\dot{\lambda} - \dot{\nu})) - \frac{e^{-\lambda}}{4} \left(2\nu'' + \nu'^2 - \lambda'\nu' + 2\frac{\nu' - \lambda'}{r} \right) \right\}, \quad (15)$$

$$\frac{(\rho + P)}{(1 - \omega^2)} \omega e^{(\nu+\lambda)/2} + e^{(\nu+\lambda)/2} \epsilon = -\frac{\dot{\lambda}}{8\pi r}. \quad (16)$$

Observe that if ν and λ are fully specified, then (13–16) becomes a system of algebraic equations for the physical variables ρ , P , ω and ϵ .

At the outside of the fluid distribution, the spacetime is that of Vaidya, given by

$$ds^2 = (1 - 2M(u)/\mathcal{R}) du^2 + 2dud\mathcal{R} - \mathcal{R}^2 (d\theta^2 + \sin^2\theta d\phi^2), \quad (17)$$

where u is a coordinate related to the retarded time, such that $u = \text{constant}$ is (asymptotically) a null cone open to the future and \mathcal{R} is a null coordinate ($g_{\mathcal{R}\mathcal{R}} = 0$). It should be remarked, however, that strictly speaking, the radiation can be considered in radial free streaming only at radial infinity.

The two coordinate systems (t, r, θ, ϕ) and $(u, \mathcal{R}, \theta, \phi)$ are related at the boundary surface and outside it by

$$u = t - r - 2M \ln \left(\frac{r}{2M} - 1 \right), \quad (18)$$

$$\mathcal{R} = r. \tag{19}$$

In order to match smoothly the two metrics above on the boundary surface $r = r_\Sigma(t)$, we must require the continuity of the first and the second fundamental form across that surface. Then it follows [11]

$$e^{\nu_\Sigma} = 1 - 2M/R_\Sigma, \tag{20}$$

$$e^{-\lambda_\Sigma} = 1 - 2M/R_\Sigma. \tag{21}$$

$$[P]_\Sigma = 0, \tag{22}$$

where, from now on, subscript Σ indicates that the quantity is evaluated at the boundary surface Σ . Next, it will be useful to calculate the radial component of the conservation law

$$T_{\nu;\mu}^\mu = 0. \tag{23}$$

where

$$T_{\mu\nu} = (\rho + P) u_\mu u_\nu - P g_{\mu\nu} + \epsilon l_\nu l_\mu \tag{24}$$

with

$$u^\mu = \left(\frac{e^{-\nu/2}}{(1 - \omega^2)^{1/2}}, \frac{\omega e^{-\lambda/2}}{(1 - \omega^2)^{1/2}}, 0, 0 \right), \tag{25}$$

$$l^\mu = (e^{-\nu/2}, e^{-\lambda/2}, 0, 0), \quad (26)$$

where u^μ denotes the four velocity of the fluid, and l^μ is a null outgoing vector.

After tedious but simple calculations we get

$$(-8\pi T_1^1)' = \frac{16\pi}{r} (T_1^1 - T_2^2) + 4\pi\nu' (T_1^1 - T_0^0) + \frac{e^{-\nu}}{r} \left(\ddot{\lambda} + \frac{\dot{\lambda}^2}{2} - \frac{\dot{\lambda}\dot{\nu}}{2} \right), \quad (27)$$

which in the static case becomes

$$P' = -\frac{\nu'}{2} (\rho + P), \quad (28)$$

which is the well known the Tolman–Oppenheimer–Volkoff equation.

3 Newtonian and Relativistic Polytrope

Although Newtonian polytropes are well known and examined in detail in most classical books on stellar structure [3], we found it worthwhile to present here the very basic facts about its theory.

3.1 The Newtonian case

As mentioned before, the theory of polytropes is based on the assumption of hydrostatic equilibrium, therefore the two starting equations are (remember that we are using geometric units)

$$\frac{dP}{dr} = -\frac{d\phi}{dr}\rho_0, \quad (29)$$

and

$$\frac{1}{r^2} \frac{d}{dr} \left(r^2 \frac{d\phi}{dr} \right) = 4\pi\rho_0, \quad (30)$$

with ϕ and ρ_0 denoting the Newtonian gravitational potential and the mass (baryonic) density, respectively.

Combining the two equation above with the polytropic equation of state

$$P = K\rho_0^\gamma = K\rho_0^{1+1/n}, \quad (31)$$

one obtains the well known Lane–Emden equation (for $\gamma \neq 1$)

$$\frac{d^2\psi_0}{d\xi^2} + \frac{2}{\xi} \frac{d\psi_0}{d\xi} + \psi_0^n = 0 \quad (32)$$

with

$$r = \xi/A_0, \quad (33)$$

$$A_0^2 = \frac{4\pi\rho_{0c}^{(n-1)/n}}{K(n+1)}, \quad (34)$$

$$\psi_0^n = \rho_0 / \rho_{0c}, \quad (35)$$

where subscript c indicates that the quantity is evaluated at the centre, and the following boundary conditions apply:

$$\frac{d\psi_0}{d\xi}(\xi = 0) = 0;$$

$$\psi_0(\xi = 0) = 1.$$

The boundary surface of the sphere is defined by $\xi = \xi_n$, such that $\psi_0(\xi_n) = 0$.

As it is well known, bounded configurations exist only for $n < 5$ and analytical solution may be found for $n = 0, 1$ and 5 .

It is also worth remembering that the polytropic equation of state may be used to model two different type of situations, namely:

- When the polytropic constant K is fixed and can be calculated from natural constants. This is the case of a completely degenerate gas in the non-relativistic ($\gamma = 5/3$; $n = 3/2$) and relativistic limit ($\gamma = 4/3$; $n = 3$).
- When K is a free parameter as for example in the case of isothermal ideal gas or in a completely convective star.

3.2 The relativistic case

When considering the polytropic equation of state within the context of general relativity, two distinct expressions are often considered. In order to avoid confusion we shall differentiate them from the beginning. Thus, the following two cases may be contemplated.

3.3 Case I

In this case the original polytropic equation of state is conserved

$$P = K\rho_0^{1+1/n}, \quad (36)$$

then it follows from the first law of thermodynamics that

$$d\left(\frac{\rho + P}{\mathcal{N}}\right) - \frac{dP}{\mathcal{N}} = Td\left(\frac{\sigma}{\mathcal{N}}\right), \quad (37)$$

where T denotes temperature, σ is entropy per unit of proper volume and \mathcal{N} is the particle density, such that

$$\rho_0 = \mathcal{N}m_0. \quad (38)$$

Then for an adiabatic process it follows

$$d\left(\frac{\rho}{\mathcal{N}}\right) + Pd\left(\frac{1}{\mathcal{N}}\right) = 0, \quad (39)$$

which together with (36) leads to

$$K\rho_0^{\gamma-2} = \frac{d(\rho/\rho_0)}{d\rho_0}, \quad (40)$$

with

$$\gamma = 1 + 1/n. \quad (41)$$

If $\gamma \neq 1$, (40) may be easily integrated to give

$$\rho = C\rho_0 + P/(\gamma - 1). \quad (42)$$

In the non-relativistic limit we should have $\rho \rightarrow \rho_0$, and therefore $C = 1$. Thus, the polytropic equation of state amounts to

$$\rho = \rho_0 + P/(\gamma - 1). \quad (43)$$

It is worth noticing that the familiar “barotropic” equation of state

$$\rho = P/(\gamma - 1), \quad (44)$$

is a particular case of (42) with $C = 0$.

In the very special case $\gamma = 1$, one obtains

$$K\rho_0^{-1} = \frac{d(\rho/\rho_0)}{d\rho_0}, \quad (45)$$

whose solution is

$$\rho = P \log \rho_0 + \rho_0 C, \quad (46)$$

or, if putting $C = 1$ from the non-relativistic limit

$$\rho = P \log \rho_0 + \rho_0. \quad (47)$$

From now on we shall only consider the $\gamma \neq 1$ case.

Next, let us introduce the following variables

$$\alpha = P_c/\rho_c, \quad (48)$$

$$r = \xi/A, \quad (49)$$

$$A^2 = 4\pi\rho_c/[\alpha(n+1)], \quad (50)$$

$$\psi_0^n = \rho_0/\rho_{0c}, \quad (51)$$

$$v(\xi) = m(r)A^3/(4\pi\rho_c), \quad (52)$$

where the mass function, as usually is defined by

$$e^{-\lambda} = 1 - 2m/r. \quad (53)$$

Then the Tolman–Oppenheimer–Volkoff equation (28) becomes

$$\xi^2 \frac{d\psi_0}{d\xi} \left(\frac{1 - 2(n+1)\alpha v/\xi}{(1-\alpha) + (n+1)\alpha\psi_0} \right) + v + \alpha\xi^3\psi_0^{n+1} = 0, \quad (54)$$

and from the definition of mass function and equation (13) in the static case,

we have

$$m' = 4\pi r^2 \rho \quad (55)$$

or

$$\frac{dv}{d\xi} = \xi^2 \psi_0^n (1 - n\alpha + n\alpha\psi_0). \quad (56)$$

In the Newtonian limit ($\alpha \rightarrow 0$), (54) and (56) become

$$\xi^2 \frac{d\psi_0}{d\xi} + v = 0 \quad (57)$$

and

$$\frac{dv}{d\xi} = \xi^2 \psi_0^n, \quad (58)$$

which are equivalent to the classical Lane–Emden equation

$$\frac{d^2\psi_0}{d\xi^2} + \frac{2}{\xi} \frac{d\psi_0}{d\xi} + \psi_0^n = 0. \quad (59)$$

3.4 Case II

Sometimes it is assumed that the relativistic polytrope is defined by

$$P = K\rho^{1+1/n}, \quad (60)$$

instead of (36). Then introducing

$$\psi^n = \rho/\rho_c, \quad (61)$$

related to ψ_0 by

$$\psi^n = \psi_0^n(1 - n\alpha + \alpha n\psi_0). \quad (62)$$

The TOV equation becomes

$$\xi^2 \frac{d\psi}{d\xi} \left(\frac{1 - 2(n+1)\alpha v/\xi}{1 + \alpha\psi} \right) + v + \alpha\xi^3 \psi^{n+1} = 0, \quad (63)$$

and from (55)

$$\frac{dv}{d\xi} = \xi^2 \psi^n. \quad (64)$$

In the Newtonian limit ($\alpha \rightarrow 0$), the Lane–Emden equation is also recovered in this case, as it should be.

Obviously both equations of state differ each other, specially in the highly relativistic regime. This can be verified by inspection of figures 1 and 2.

4 The method

Let us now give a brief resume of the method we shall use to describe the evolution of the relativistic polytrope. However before doing so some general considerations will be necessary.

4.1 Equilibrium and quasi–equilibrium

The simplest situation, when dealing with self–gravitating spheres, is that of equilibrium (static case). In our notation that means that $\omega = \epsilon = 0$, all time derivatives vanishes, and we obtain the generalized Tolman–Oppenheimer–Volkoff equation (28).

Next, we have the quasistatic regime. By this we mean that the sphere changes slowly, on a time scale that is very long compared to the typical time in which the sphere reacts to a slight perturbation of hydrostatic equilibrium,

this typical time scale is called hydrostatic time scale [3] (sometimes this time scale is also referred to as dynamical time scale, e.g. see [21]). Thus, in this regime the system is always very close to hydrostatic equilibrium and its evolution may be regarded as a sequence of static models linked by (16). This assumption is very sensible because the hydrostatic time scale is very small for many phases of the life of the star. It is of the order of 27 minutes for the Sun, 4.5 seconds for a white dwarf and 10^{-4} seconds for a neutron star of one solar mass and 10 Km radius. It is well known that any of the stellar configurations mentioned above, generally, change on a time scale that is very long compared to their respective hydrostatic time scales.

However, as already mentioned, in some important cases, this approximation is not longer reliable, and one needs to consider departures from quasi-equilibrium. We shall describe such departures, in the post-quasi-static approximation defined below.

4.2 The effective variables and the post-quasistatic approximation

Let us now define the following effective variables:

$$\tilde{\rho} = T_0^0 = \frac{\rho + P\omega^2}{1 - \omega^2} + \epsilon, \quad (65)$$

$$\tilde{P} = -T_1^1 = \frac{P + \rho\omega^2}{1 - \omega^2} + \epsilon. \quad (66)$$

In the quasistatic regime the effective variables satisfy the same equation (28) as the corresponding physical variables (taking into account the contribution of ϵ to the “total” energy density and radial pressure, whenever the free streaming approximation is being used). Therefore in the quasistatic situation (and obviously in the static too), effective and physical variables share the same radial dependence. Next, feeding back (65) and (66) into (13) and (14), these two equations may be formally integrated, to obtain:

$$m = 4\pi \int_0^r r^2 \tilde{\rho} dr, \quad (67)$$

$$\nu = \nu_\Sigma + \int_{r_\Sigma}^r \frac{2(4\pi r^3 \tilde{P} + m)}{r(r - 2m)} dr. \quad (68)$$

From where it is obvious that for a given radial dependence of the effective variables, the radial dependence of metric functions becomes completely determined.

With this last comment in mind, we shall define the post-quasistatic regime as that corresponding to a system out of equilibrium (or quasiequilibrium) but whose effective variables share the same radial dependence as the

corresponding physical variables in the state of equilibrium (or quasiequilibrium). Alternatively it may be said that the system in the post–quasistatic regime is characterized by metric functions whose radial dependence is the same as the metric functions corresponding to the static (quasistatic) regime. The rationale behind this definition is not difficult to grasp: we look for a regime which although out of equilibrium, represents the closest possible situation to a quasistatic evolution (see more on this point in the last Section).

4.3 The algorithm

Let us now outline the approach that we shall use:

1. Take an interior solution to Einstein equations, representing a fluid distribution of matter in equilibrium, with a given

$$\rho_{st} = \rho(r); \quad P_{st} = P(r).$$

This static solution will be obtained in this work by integration of the relativistic Lane–Emden equations (54), (56) or (63), (64).

2. Assume that the r dependence of \tilde{P} and $\tilde{\rho}$ is the same as that of P_{st} and ρ_{st} , respectively.
3. Using equations (67) and (68), with the r dependence of \tilde{P} and $\tilde{\rho}$, one gets m and ν up to some functions of t , which will be specified below.

4. For these functions of t one has three ordinary differential equations (hereafter referred to as surface equations), namely:
 - (a) Equation (12) evaluated on $r = r_\Sigma$.
 - (b) The equation relating the total mass loss rate with the energy flux through the boundary surface.
 - (c) Equation (27) evaluated on $r = r_\Sigma$.
5. The system of surface equations described above may be closed with the additional information about some of the physical variables evaluated on the boundary surface (e.g. the luminosity).
6. Once the system of surface equations is closed, it may be integrated for any particular initial data.
7. Feeding back the result of integration in the expressions for m and ν , these two functions are completely determined.
8. With the input from the point 7 above, and remembering that once metric functions are fully specified, field equations become an algebraic system of equations for the physical variables; these may be found for any piece of matter distribution.

4.4 The Surface equations

As it should be clear from the above, the crucial point in the algorithm is the system of surface equations. So, let us specify them now.

Introducing the dimensionless variables

$$A = r_\Sigma/m_\Sigma(0),$$

$$F = 1 - 2M/A,$$

$$M = m_\Sigma/m_\Sigma(0),$$

$$\Omega = \omega_\Sigma,$$

$$\beta = t/m_\Sigma(0),$$

where $m_\Sigma(0)$ denotes the total initial mass, we obtain the first surface equation by evaluating (12) at $r = r_\Sigma$. Thus, one gets

$$\frac{dA}{d\beta} = F\Omega. \tag{69}$$

Next, using junction conditions, one obtains from (53), (13) and (16) evaluated at $r = r_\Sigma$, that

$$\frac{dM}{d\beta} = -F(1 + \Omega)\hat{E}, \tag{70}$$

with

$$\hat{E} = 4\pi r_\Sigma^2 \hat{\epsilon}_\Sigma, \tag{71}$$

where the first and second term on the right of (70) represent the gravitational redshift and the Doppler shift corrections, respectively.

Then, defining the luminosity perceived by an observer at infinity as

$$L = -\frac{dM}{d\beta}.$$

we obtain the second surface equation in the form

$$\frac{dF}{d\beta} = \frac{F}{A}(1 - F)\Omega + 2L/A. \quad (72)$$

The third surface equation may be obtained by evaluating at the boundary surface the conservation law $T_{1;\mu}^\mu = 0$, which reads

$$\begin{aligned} & \tilde{P}' + \frac{(\tilde{\rho} + \tilde{P})(4\pi r^3 \tilde{P} + m)}{r(r - 2m)} = \\ & \frac{e^{-\nu}}{4\pi r(r - 2m)} \left(\ddot{m} + \frac{3\dot{m}^2}{r - 2m} - \frac{\dot{m}\dot{\nu}}{2} \right) + \frac{2}{r}(P - \tilde{P}). \end{aligned} \quad (73)$$

In the case when the effective density is separable, i.e., $\tilde{\rho} = \mathcal{F}(t)\mathcal{H}(r)$; equation (73) evaluated at the boundary surface leads to

$$\begin{aligned} \frac{d\Omega}{d\beta} = \Omega^2 & \left[\frac{8F}{A} + 2F\mathcal{K}(r_\Sigma) + 4\pi\tilde{\rho}_\Sigma A(3 - \Omega^2) \right] \\ & - \frac{F}{\tilde{\rho}_\Sigma} \left[R + \frac{2}{A} \left(\tilde{\rho}_\Sigma \Omega^2 + \frac{\bar{E}(1 + \Omega)}{4\pi r_\Sigma^2} \right) \right], \end{aligned} \quad (74)$$

where

$$R = \left[\tilde{P}' + \frac{\tilde{P} + \tilde{\rho}}{1 - 2m/r} (4\pi r \tilde{P} + \frac{m}{r^2}) \right]_\Sigma, \quad (75)$$

$$\bar{E} = \hat{E}(1 + \Omega) \quad (76)$$

and

$$\mathcal{K}(r_\Sigma) = \frac{d}{dr_\Sigma} \ln \left(\frac{1}{r_\Sigma} \int_0^{r_\Sigma} dr r^2 \mathcal{H}(r) / \mathcal{H}(r_\Sigma) \right). \quad (77)$$

Before analyzing specific models, some interesting conclusions can be obtained at this level of generality. One of these conclusions concerns the condition of bouncing at the surface which, of course, is related to the occurrence of a minimum radius A . According to (69) this requires $\Omega = 0$, and we have

$$\frac{d^2 A}{d\beta^2} = F \frac{d\Omega}{d\beta}, \quad (78)$$

or using (74)

$$\frac{d\Omega}{d\beta}(\Omega = 0) = -\frac{F}{\tilde{\rho}_\Sigma} \left[R + \frac{2\hat{E}}{4\pi r_\Sigma^2 A} \right]. \quad (79)$$

Observe that a positive energy flux (\hat{E}) tends to decrease the radius of the sphere, i.e., it favors the compactification of the object, which is easily understood. The same happens when $R > 0$. The opposite effect occurs when these quantities have the opposite signs. Now, for a positive energy flux the sphere can only bounce at its surface when

$$\frac{d\Omega}{d\beta}(\Omega = 0) \geq 0.$$

According to (79) this requires

$$-R(\Omega = 0) \geq 0. \tag{80}$$

A physical meaning can be associated to this equation as follows. For non-radiating, static configuration, R as defined by (75) consists of two parts. The first term which represents the hydrodynamical force (see (28)) and the second which is of course the gravitational force. The resulting force in the sense of increasing r is precisely $-R$, if this is positive a net outward acceleration occurs and vice-versa. Equation (80) is the natural generalization of this result for general non-static configurations.

5 Models and their numerical implementation

5.1 Effective variables

Once the profiles of energy density and pressure have been established in the static case via the integration of the corresponding Lane–Emden equations, we proceed with the determination of effective variables according to the algorithm sketched above. However, as it should be clear such determination is not unique. The following possibilities arise:

1. $\tilde{\rho} = f(t) + h(r)$ $\tilde{p} = g(t) + i(r)$, where $h(r)$ and $i(r)$ correspond to the pressure and total energy density obtained from the integration of

the relativistic Lane–Emden equations, in both cases described above.

However this model has not static limit.

2. $\tilde{\rho} = f(t)h(r)$ and $\tilde{p} = g(t) + K\tilde{\rho}_0^{1+1/n}$, for the case I, where $\tilde{\rho}_0 = f(t)h_0(r)$, being $h_0(r)$ the baryonic mass density in the static limit; $\tilde{p} = g(t) + K\tilde{\rho}^{1+1/n}$, for the case II. In both cases $K = K(m_\Sigma, r_\Sigma)$.

On what follows we shall consider only the possibility 1 above.

5.2 Numerical implementation of models

We have used an standard Runge–Kutta routine to obtain functions $h(r)$, $h_0(r)$ and $i(r)$ from the integration of relativistic Lane–Emden equations for different values of n and α . Integration was performed from $\xi = 0$ until the first zero of ψ (or ψ_0).

Next, for the third surface equation we need to calculate numerically the following terms:

$$\left[\frac{di(r)}{dr} \right]_{r=r_\Sigma}, \quad (81)$$

$$k(t) = \int_0^{r_\Sigma} r^2 h(r) dr. \quad (82)$$

Observe that $dk(t)/dt = 0$, since $h(r_\Sigma) = 0$.

For the calculation of (81) and (82) we have adjusted a Chebyshev polynomial [22] to functions $h(r)$ and $i(r)$. Also, for the calculation of either of

these functions in the Chebyshev's nodes or within different interior regions we have used the interpolating Lagrange polynomials.

A standard Runge–Kutta method has also been applied to solve surface equations. These three equations are solved as an initial value problem, upon specification of $A(t = 0)$, $F(t = 0)$ and one function of u . Specifically we choose

$$L = \frac{2m_R}{\sqrt{\pi}} e^{-4(t-5/2)^2},$$

where m_R is the mass to be radiated.

Once the surface equations have been integrated, we proceed to calculate the metric functions and their derivatives. For doing so, we need to calculate numerically the following expressions:

$$\frac{di(r)}{dr}, \tag{83}$$

$$\int_0^r r^2 h(r) dr, \tag{84}$$

$$\int_a^r \frac{2(4\pi r^3 \tilde{p} + m)}{r(r - 2m)} dr \tag{85}$$

and

$$\int_a^r \frac{\partial}{\partial t} \left\{ \frac{2(4\pi r^3 \tilde{p} + m)}{r(r - 2m)} \right\} dr. \tag{86}$$

Where the last expression appears in the equation for the time derivative of ν given by

$$\dot{\nu} = \dot{\nu}_\Sigma + \int_{r_\Sigma(t)}^r \frac{\partial}{\partial t} \left\{ \frac{2(4\pi r^3 \tilde{p} + m)}{r(r - 2m)} \right\} dr - \left\{ \frac{2(4\pi r^3 \tilde{p} + m)}{r(r - 2m)} \right\}_{r_\Sigma(t)} \dot{r}_\Sigma$$

For the numerical integration of (85) and (86) it is necessary to calculate the integrands on points of the lattice defined in the integration of Lane–Emden equation, using again the Chebyshev’s polynomials and Lagrange interpolants. Once the metric functions and their derivatives have been completely determined, we use the field equations to obtain algebraically the physical variables.

All along evolution we keep radial dependence obtained from the solution of the Lane–Emden equations. This was implemented fitting the $h(r)$ and $i(r)$ profiles to the radius’s distribution at time t . Thus, the radial coordinate is scaled by means of:

$$r \rightarrow \left(\frac{r_{\Sigma}(t)}{r_{\Sigma}(0)} \right) r.$$

The developed code was paralelized using MPI routines for FORTRAN. We use as many nodes as interior regions studied. One typical run takes, for one region and one time unit, one a half hour in a 900 MHz. central processing unit.

5.3 Models

Although a large number of models has been worked out, we shall present here only two for illustration, corresponding to the cases I and II. Both were calculated for values: $n = 2$, $\alpha = 0.1$, $\Omega(0) = -0.05$, with an emission of

0.01 of the initial mass. The profiles of physical variables are exhibited in figures 3–6. As we increase the emission we arrive at a point where case II becomes unphysical before case I. If we increase n , for both cases, the initial distribution is less compact. On the contrary, if we increase α the initial distribution is more compact. Figure 7 shows the normalized radii evolution for both cases, different values of n and $\alpha = 0.1$.

6 Conclusions

We have considered two possible definitions of relativistic polytrope and have presented a method to study their evolution. The models represent a generalization of the static polytrope to the case of evolving and dissipating fluid spheres, which in the static limit satisfy a polytropic equation of state. This allows for modeling self-gravitating objects, and at the same time brings out differences between the two possible definitions of polytropes, considered here. We have incorporated dissipation, a fundamental process in the process of gravitational collapse, into discussion. It remains, to consider the diffusion limit, however because of the additional complication associated to the necessity of introducing an equation of transport, we have only considered here the simplest, streaming out limit.

Although the examples are presented with the sole purpose of illustrating

the method (our main goal here being to provide a tool for modeling the evolution of relativistic polytropes), some comments on them, are in order.

The difference between the two definitions of polytrope considered here, are clearly exhibited in figures 1–2. To magnify such difference we present the results corresponding to the “ultra-relativistic” case ($\alpha = 1$). As can be seen, for $n \leq 1.365$, configurations of case I have smaller radii than those corresponding to the case II. This situation reverses for $n > 1.365$. In general, bounded relativistic configurations exist for smaller values of n , than in the Newtonian case.

Figures 3–6 show how differently, both polytropes evolve. As it appears from these figures, the case II leads to a stronger collapse. This tendency is confirmed by curves $c - d$ of figure 7. Also, curves $a - b$ on this same figure show an example of bouncing for $n = 2.5$. The strongest bouncing of case I, further indicates that the equation of state resulting from case I is stiffer than the obtained from case II. It is worth mentioning that these differences are observed in a large number of models, for a wide range of values of n , α and initial data.

Acknowledgements

WB was benefited from research support from FONACIT under grant S1-98003270. Computer time for this work was provided by the Centro Nacional de Cálculo Científico de la Universidad de los Andes (CeCalcULA).

References

- [1] S. Chandrasekhar, *An Introduction to the Study of Stellar Structure*, (University of Chicago Press, Chicago) (1939).
- [2] S.L. Shapiro and S.A. Teukolsky, *Black Holes, White Dwarfs and Neutron Stars*, (John Wiley and Sons, New York) (1983).
- [3] R. Kippenhahn and A. Weigert, *Stellar Structure and Evolution*, (Springer Verlag, Berlin) (1990).
- [4] R. Tooper, *Astrophys J.*, **140**, 434 (1964); *ibid*, **142**, 1541 (1965); *ibid*, **143**, 465 (1966).
- [5] S. Bludman, *Astrophys J.*, **183**, 637 (1973).
- [6] U. Nilsson and C. Uggla, *preprint gr-qc/0002022*.
- [7] H. Maeda, T. Harada, H. Iguchi and N. Okuyama, *preprint gr-qc/0204039*.

- [8] P. Goldreich and S. Weber, *Astrophys J.*, **238**, 991 (1980)
- [9] I. Iben, *Astrophys. J.* **138**, 1090, (1963).
- [10] E. Myra and A. Burrows, *Astrophys. J.* **364**, 222 (1990).
- [11] L. Herrera, W. Barreto, A. Di Prisco and N.O. Santos, *Phys. Rev. D* **65**, 104004 (2002).
- [12] L. Lenher, Preprint *gr-qc/0106072*,1 (2001).
- [13] M. W. Choptuik, *Phys. Rev. Lett.*, **70**, 9 (1993).
- [14] J. A. Font, *Living Rev. Rel.*, **47**, 2 (2000).
- [15] J. Winicour, *Living Rev. Rel.*, **1**, 5 (1998).
- [16] D. Kazanas and D. Schramm, *Sources of Gravitational Radiation*, L. Smarr ed., (Cambridge University Press, Cambridge, 1979).
- [17] W. D. Arnett, *Astrophys. J.* , **218**, 815 (1977).
- [18] D. Kazanas, *Astrophys. J.* , **222**, 2109 (1978).
- [19] J. Lattimer, *Nucl. Phys.*, **A478**, 199 (1988).
- [20] H. Bondi, *Proc. R. Soc. London*, **A281**, 39 (1964)

- [21] C. Hansen and S. Kawaler, *Stellar Interiors: Physical principles, Structure and Evolution*, (Springer Verlag, Berlin) (1994).
- [22] W. H. Press, S. A. Teukolsky, W. T. Vetterling y B. P. Flannery, *Numerical Recipes, Second Ed.* Cambridge University Press (1992).

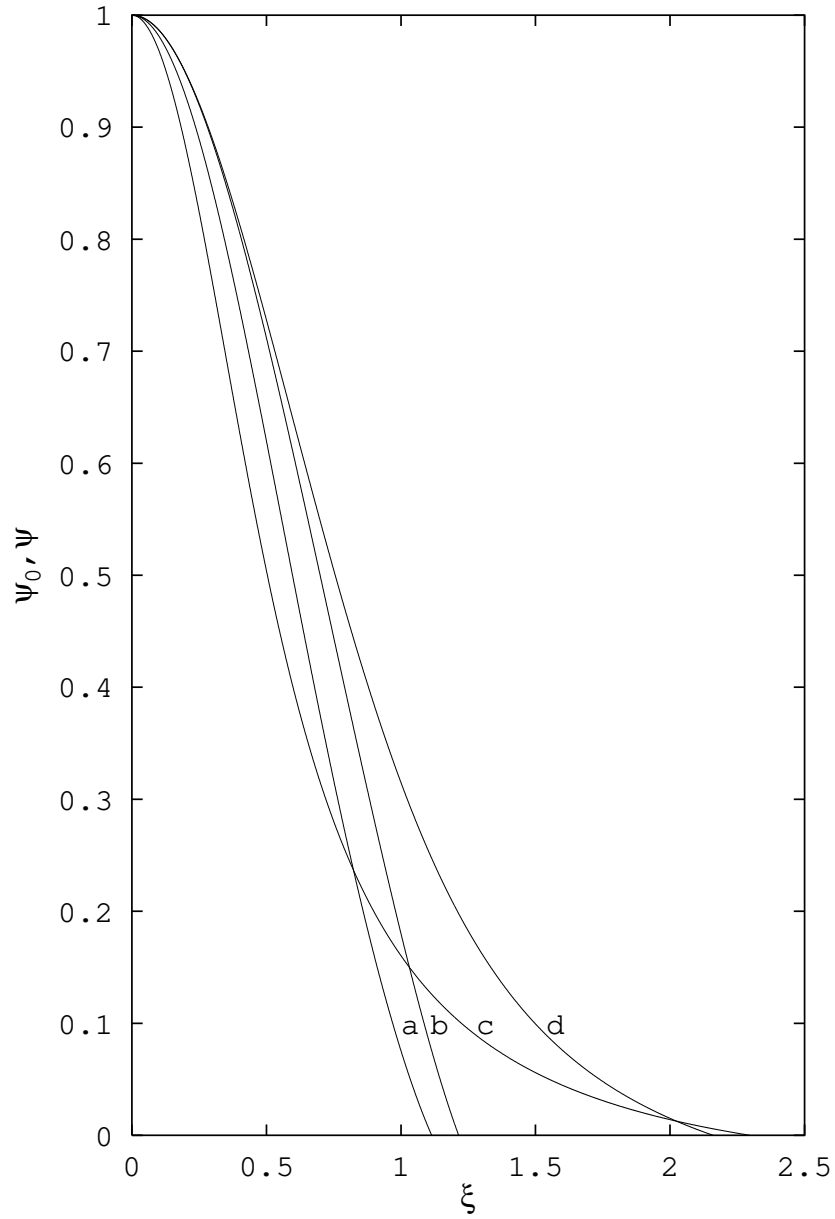


Figure 1: ψ_0 (Case I) and ψ (Case II) as a function of ξ for $\alpha = 1$ and different values of n : (a) Case I, $n = 0.5$; (b) Case II, $n = 0.5$; (c) Case I, $n = 1.5$; (d) Case II, $n = 1.5$.

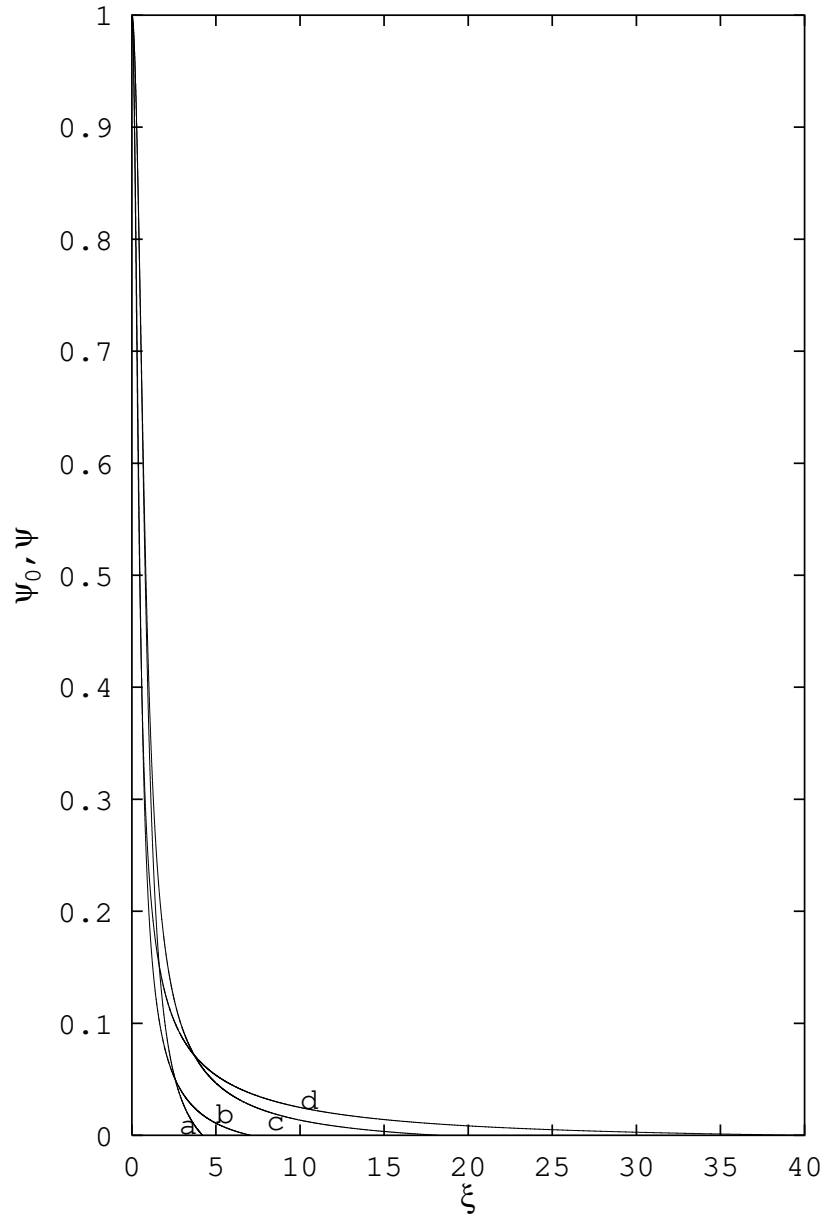


Figure 2: ψ_0 (Case I) and ψ (Case II) as a function of ξ for $\alpha = 1$ and different values of n : (a) Case II, $n = 2$; (b) Case I, $n = 2$; (c) Case II, $n = 2.5$; (d) Case I, $n = 2.5$.

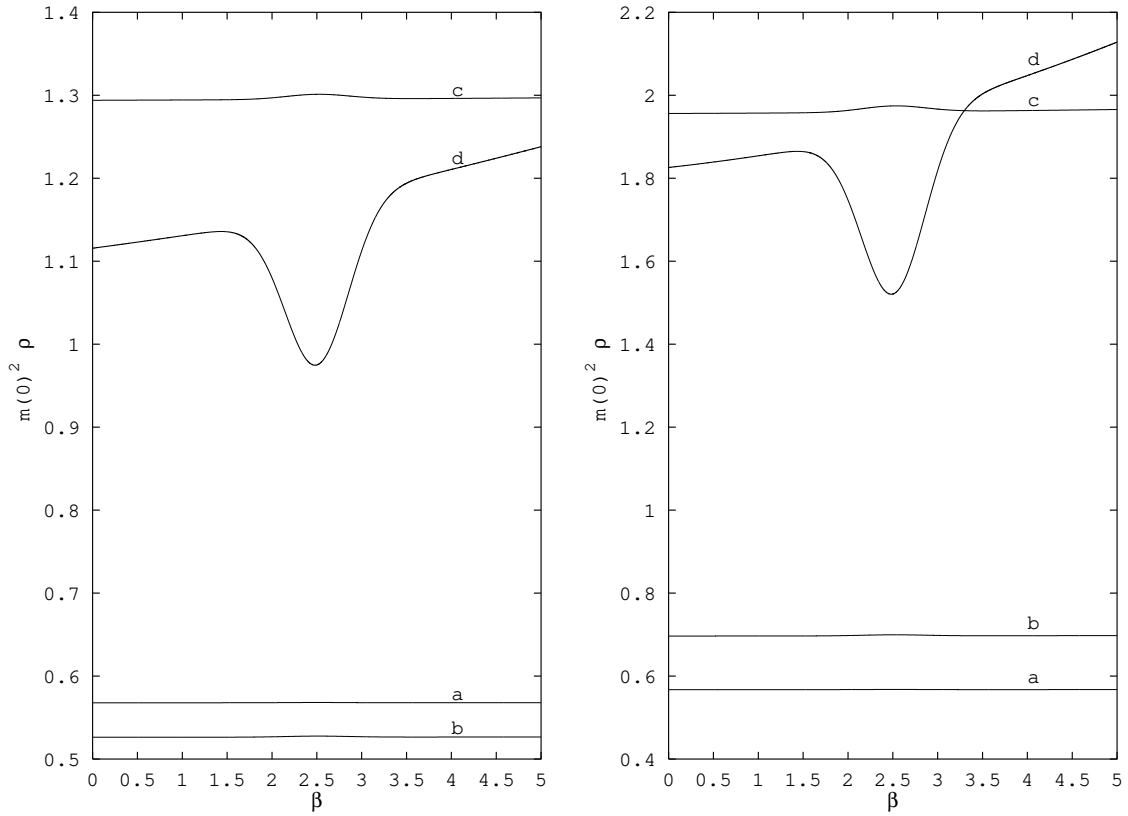


Figure 3: Adimensional energy density (Case I to the left; Case II to the right) as a function of dimensionless time for $n = 2$ and $\alpha = 0.1$ at different regions: (a) $r/a = 0.25$ (multiplied by 10); (b) $r/a = 0.50$ (multiplied by 10); (c) $r/a = 0.75$ (multiplied by 10^2); (d) $r/a = 1.00$ (multiplied by 10^4).

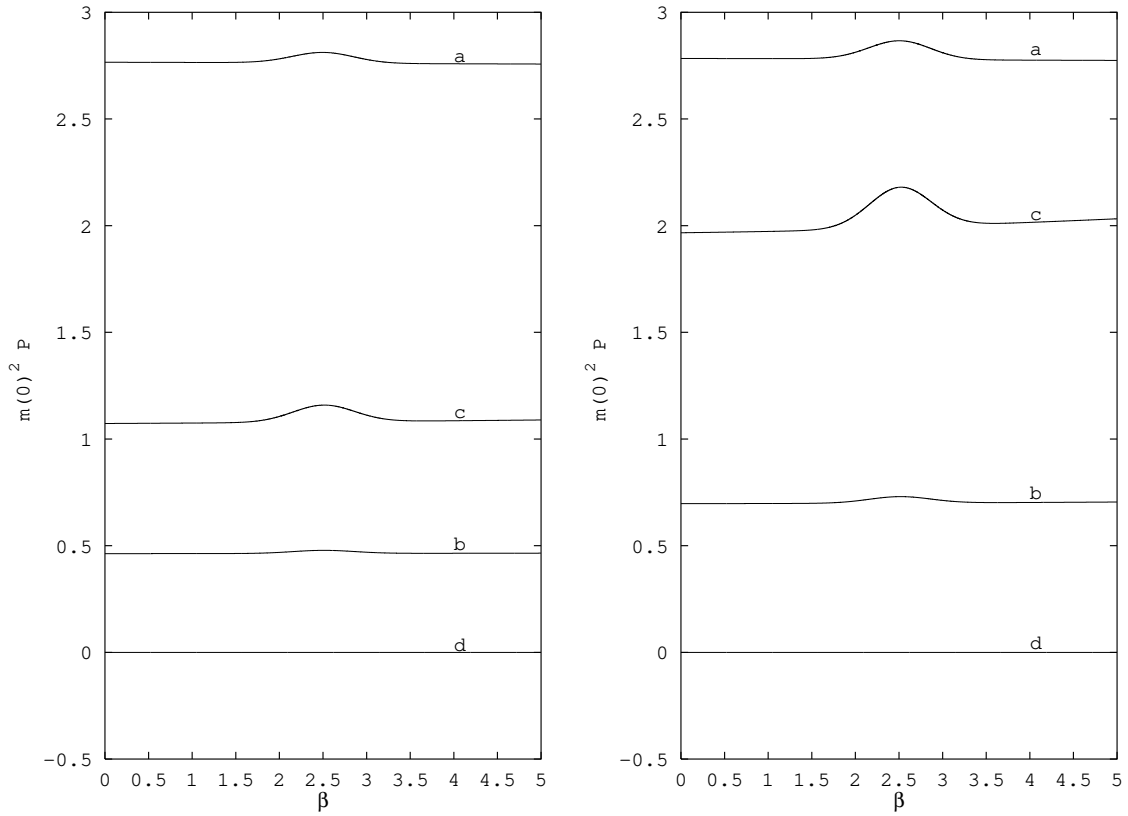


Figure 4: Adimensional pressure (Case I to the left; Case II to the right) as a function of dimensionless time for $n = 2$ and $\alpha = 0.1$ at different regions: (a) $r/a = 0.25$ (multiplied by 10^3); (b) $r/a = 0.50$ (multiplied by 10^2); (c) $r/a = 0.75$ (multiplied by 10^3); (d) $r/a = 1.00$.

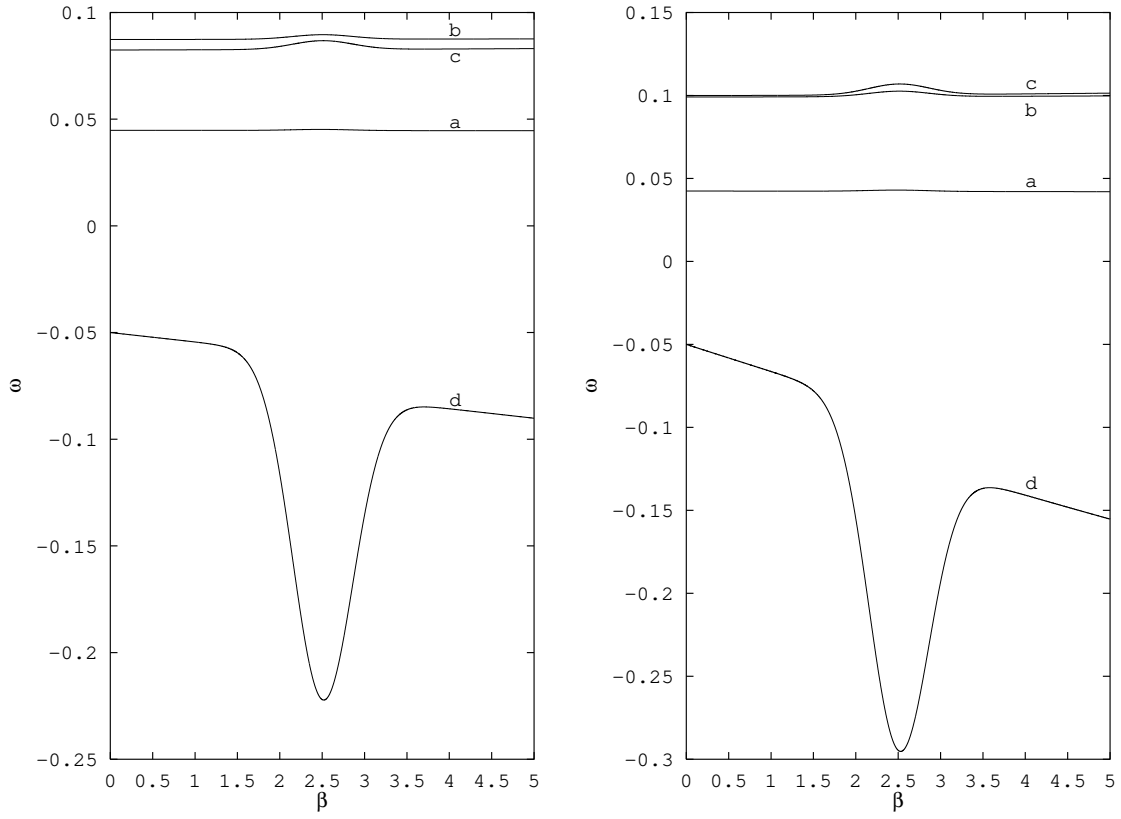


Figure 5: Radial velocity (Case I to the left; Case II to the right) as a function of dimensionless time for $n = 2$ and $\alpha = 0.1$ at different regions: (a) $r/a = 0.25$; (b) $r/a = 0.50$; (c) $r/a = 0.75$; (d) $r/a = 1.00$.

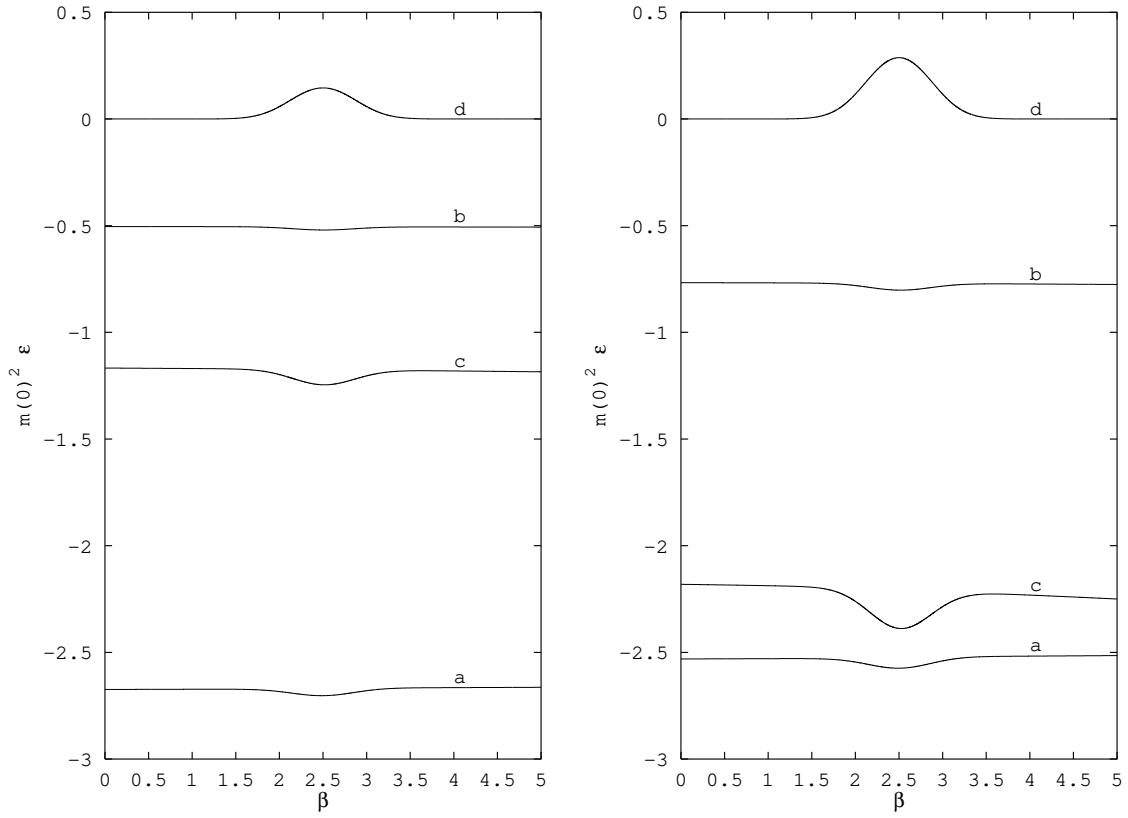


Figure 6: Adimensional flux of energy (Case I to the left; Case II to the right) as a function of dimensionless time for $n = 2$ and $\alpha = 0.1$ at different regions: (a) $r/a = 0.25$ (multiplied by 10^3); (b) $r/a = 0.50$ (multiplied by 10^2); (c) $r/a = 0.75$ (multiplied by 10^3); (d) $r/a = 1.00$ (multiplied by 10^4).

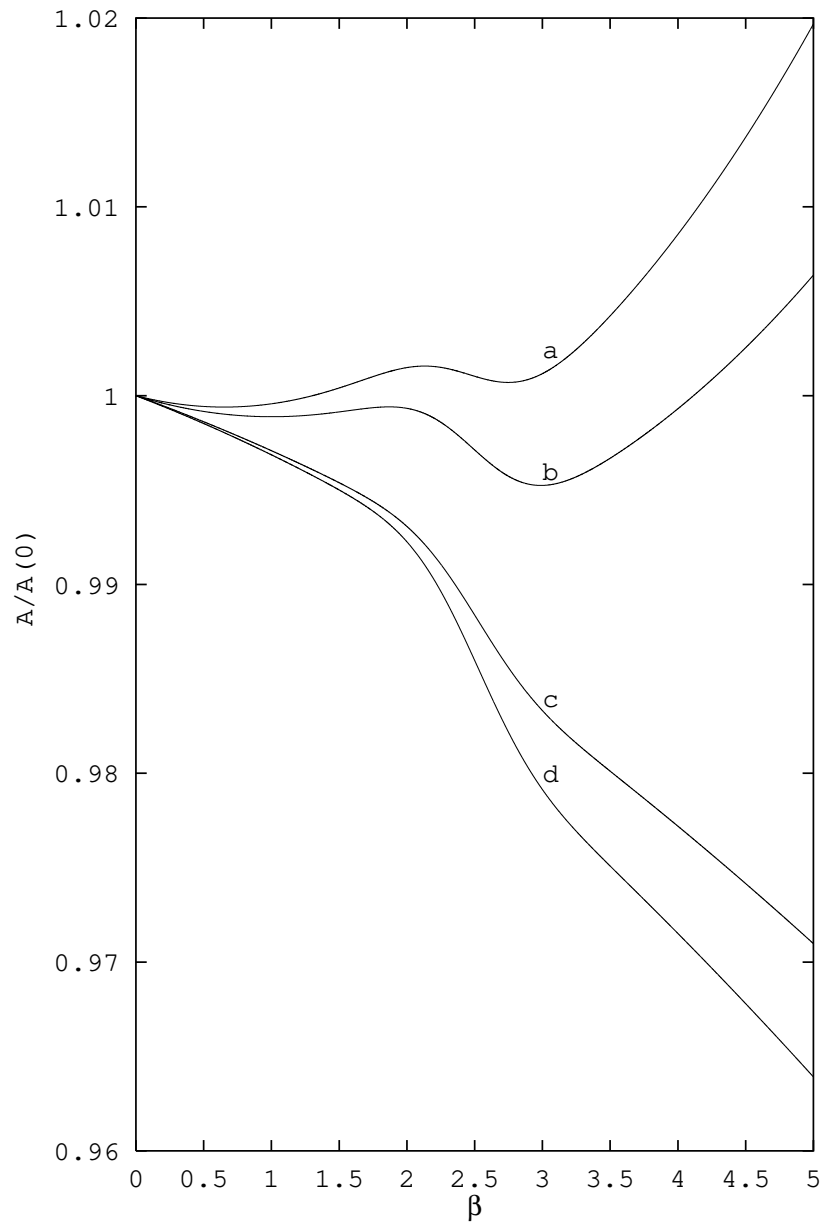


Figure 7: Evolution of the normalized radii for $\alpha = 0.1$, both cases and different values of n : (a) Case I, $n = 2.5$; (b) Case II, $n = 2.5$; (c) Case I, $n = 1.5$; (d) Case II, $n = 1.5$.